

Inside the Neutron

Calculation of the mass and β -decay-curve of the Neutron

by Norbert Buchholz

Abstract

In this work we have used the classical neutron model of proton and nuclear electron in combination with the findings of projection theory, according to which the neutron is a cube and its interior lies below the spatial resolution, where the physical laws of our space-time world only apply to a limited extent and consequently the objections raised against this model by established physics do not apply.

The electron does not reside in the entire cubic interior, but in a potential sphere ($r = 6.355181 \cdot 10^{-16} \text{ m}$) around the positron. This potential space is statistically occupied by the electron by random jumps with a jump duration of t_{\min} .

From the statistical frequency of the individual potential energies, the mean mass of the neutron was calculated to be $1.674927328 \cdot 10^{-27} \text{ kg}$. The potential jumps mentioned above lead to a change in the size of the neutron at a constant elementary particle density in the rhythm of the jumps (oscillation model). The β -decay is caused by jumps of the electron to the outer surface of the neutron, where they are ejected from the neutron by membrane oscillation, whereby only $1/6$ of the oscillation energy is transferred to the electron as kinetic energy. This is the real secret of the missing energy in the decay spectrum of the neutron. Two curves were constructed to calculate the decay curve. The base curve reflects the energetic and geometric conditions in the potential space of the electron, while the second, the jump curve, takes into account the individual jumps to the respective points on the neutron surface. The superposition of these two curves resulted in a curve that is in excellent agreement with the experimentally determined curves, in which the irregular curve progression at the maximum of the measurement curves is also very well reproduced, which to our knowledge is not the case with the calculations of established physicists. Neutrinos are not required in our obviously accurate model. In the last section, the conversion factor between time and length was calculated as $1 \text{ m}^{4/3}/\text{s}$ for the interior of the neutron. This contradicts the calculations of the same factor for the world outside the neutron with $61.66801 \text{ m}^{4/3}/\text{s}$, which impressively confirms our initial hypothesis of deviating physics inside the neutron.

A Introduction

In the projection theory⁴, the cubic three-dimensional space portion of the space-time pixel is also the volume of the proton. As its specific acceleration, we obtain a hypothetical particle that we want to call a graviton. Together with the electric elementary particles positron and electron, this results in an extremely simple "elementary particle zoo"

$$\text{Space-time pixel} = s_{\min}^3 t_{\min}$$

$$\text{Space pixel} = s_{\min}^3$$

Space pixel x acceleration = graviton
 Graviton + positron = proton
 Graviton + positron + nuclear electron = neutron

Until E Fermi's work on β -decay in 1934, the structure of the neutron from positrons and core electrons, as postulated above, was the consensus among theoretical physicists. A model that is in excellent agreement with the charge distribution in the neutron determined by analyzing form factors (see Fig. 1).

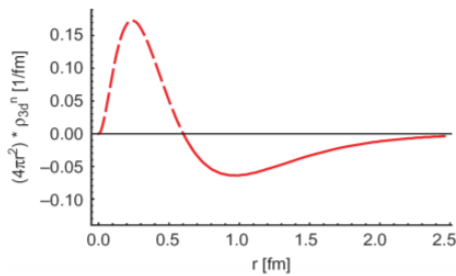


Fig. 1 Charge distribution in the neutron ¹

Fermi, on the other hand, postulated a non-composite, neutral particle and assumed that the decay products electrons and neutrinos are formed spontaneously from nothing through the interaction of special fields during β -decay.

The latter view is still valid today, although according to the theory currently favored by physicists, the quark-gluon theory, the neutron again consists of differently charged particles, i.e. an up quark ($2/3e^+$) and two down quarks ($2 \times 1/3 e^-$), i.e. as in the positron-core electron model, equal proportions of opposite charges that neutralize each other in the external effect. For the observed charge distribution in the neutron, the quark model postulates a temporal and spatial unequal distribution of the negative and positive components.

While the decay of a neutron into electrons and protons - neutrinos as pure fiction, as we will prove in this work, play no **role** for us - can be clearly described and understood according to the classical model as a simple separation process, the generation of elementary particles that are not even present in the initial particle seems to be quite inexplicable, not to say mysterious. As a rule, it is also not assumed that the rabbit in a magician's top hat actually materializes out of nowhere - as the illusionist would like us to believe - but is already a hidden reality, well concealed from our eyes, and only needs to be conjured out of a hat.

We thus also return to the original model of the neutron consisting of proton and core electron, although this can hardly be maintained from the perspective of Bohr's model for hydrogen, for example, since the lowest orbital radius of approx. 10^{-11} m inside the neutron would shrink to approx. 10^{-15} m and thus the original orbital velocity of $c/137$ would inevitably have to increase to many thousands of times, i.e. to a multiple of the speed of light.

However, what completely changes the situation is the fact that inside a neutron we are no longer moving in a well-defined space, as we are in a spatial pixel, i.e. below the spatial resolution, where analogous to the pixels of our electronic photography it is no longer possible to determine the exact location of the particles inside. Overall, we must assume that our established physics only applies to a limited extent inside the neutron.

B The calculation of the mass and the β -decay curve of the neutron

a) Calculation of the mass of the neutron

1) The jump theory

However, the lack of spatial resolution inside the neutron shown above does not mean that the electron degenerates into a space-filling structure, as it must be taken into account that the temporal resolution is still far from being undercut. This is greater than the lateral resolution by the amount of c , so that we can assume that the processes are precisely determined in time.

S_{Pix} : Number of smallest lengths s_{min} per unit length s_E

t_{pix} : Number of minimum times t_{min} per unit time t_E

$$t_{pix} = \frac{t_E}{t_{min}} = 2,26873 \cdot 10^{23}$$

$$S_{pix} = \frac{s_E}{s_{min}} = 7,567674 \cdot 10^{14}$$

$$\frac{t_{pix}}{S_{pix}} = |c|$$

We therefore assume that all positions of the available space are statistically occupied by random jumps of the electron, with each jump taking place in the minimum time t_{min}

In a first approach, we assume that the available space is given by the cube of the neutron. Of course, the electron can occupy any position, i.e. positions that are arbitrarily close to each other. In this case, however, the overlapping volumes must be subtracted, so that ultimately only the positions that lead to a complete filling of space are relevant.

According to projection theory, a constant elementary particle density is given, i.e. the following applies:

$$k_{pe} = \frac{m_p}{m_e} = \frac{V_p}{V_e} = N_j = 1836,152$$

This means that k_{pe} is not only the known mass ratio but also the volume ratio of proton and electron. According to our new considerations outlined above, k_{pe} also indicates how many jumps (N_j) are required for a space-filling occupation of the proton with electrons. The jump time was initially set quite arbitrarily to t_{min} , but this turned out to be a very useful approach in the course of the calculations.

We can thus calculate the time for a space-filling occupation of the proton volume with electrons, which we will refer to below as the period (t_{per}).

The following applies in general:

$$t_{per} = N_j t_{min}$$

$$t_{per_k} = k_{pe} t_{min} = 8,09329979 \cdot 10^{-21} [s]$$

For the following calculation, it is initially only important to know the relation

$$s_x^{\frac{4}{3}} = t_x \quad (s)$$

and the inverse function

$$t_x^{\frac{3}{4}} = s_x \quad (m)$$

and to accept them uncritically for the time being, although of course the simple conversion of length into time and vice versa causes every experienced physicist great discomfort. We will return to this very important topic in detail in the final section of this paper.

We now convert the period duration determined via k_{pe} into a length which, according to our assumption, has a certain relevance as the distance of the electron from the center.

$$t_{per_k}^{\frac{3}{4}} = s_x = (8,09329979 \cdot 10^{-21})^{\frac{3}{4}} [m]$$

$$s_x = 8,532852153 \cdot 10^{-16} [m]$$

The value for s_x alone, however, was not useful. For previously unknown reasons, it had to be extended by the radius of the electron r_e .

$$s_x + r_e = 9,202285104 \cdot 10^{-16} [m]$$

If the length found above is used as the distance from the center of mass of an electron to the center of the neutron, the corresponding mass is obtained from the resulting potential energy via c^2 and the mass of the neutron is obtained by adding the proton and electron mass. The result can be classified as excellent with a relative error of $6.5 \cdot 10^{-8}$

$$m_N = \frac{e^2}{8\pi\epsilon_0 c^2 (s_x + r_e)} + m_p + m_e = 1,674927607^{-27} [kg]$$

$$m_{N_{lit}} = 1,674927498 \cdot 10^{-27} kg$$

$$\Delta_{rel} = 6,5 \cdot 10^{-8}$$

The mathematical result is excellent, but the resulting model is not suitable for constructing a meaningful structure of the neutron. This is because the calculated radius of $9.20228 \cdot 10^{-16} m$ for the spherical surface on which the electron would have to reside exclusively (symbolized by the light grey circle in Fig. 2) is only slightly less than the length of half the surface diagonal FD (red straight line in Fig. 2), i.e. the calculated spherical surface lies almost completely outside the neutron. What is astonishing about this calculation is that the fictitious assumption of a space-filling electron leads to a fictitious solution which, however, mathematically reflects the mass of the neutron very accurately.

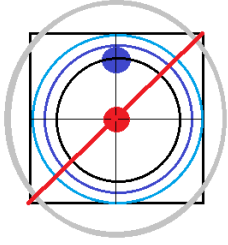


Fig. 2 Schematic two-dimensional representation of the neutron (not to scale)

2) The calculation of the residence space of the electron in the neutron

N_j indicates not only the number of jumps required to fill a certain volume with electrons, but also the number of electron volumes that fill this space. So it is not only as mentioned above

$$t_{per} = N_j t_{min}$$

but also

$$V_x = N_j V_e$$

The best-known example of this is:

$$N_j = k_{pe}$$

$$V_p = N_j V_e$$

We will need this relationship for the following calculations. First, however, we had to find a special length that was not chosen arbitrarily. This was achieved with the mean value of the electron radius and the edge length of the proton. We have thus combined two of the most important quantities of this system into one.

$$s_x = \sqrt{r_e s_{min}} [m]$$

However, for whatever reason, this value still had to be multiplied by Φ in order to produce meaningful results.

$$s_{x_2} = \sqrt{r_e s_{min}} \Phi$$

$$\Phi = 1,61803389$$

Using the relationship known from projection theory

$$s_{min} = 2\pi^2 r_e$$

we obtain from the above equation for s_{x_2} a very interesting combination of all relevant basic variables of the projection system, such as r_e , π and Φ

$$s_{x_2} = \Phi \cdot \pi \cdot r_e \cdot \sqrt{2} = 4,81238 \cdot 10^{-16} [m]$$

We now transform the length into a time, which we assume to be a period duration.

$$t_{per} = \left(\Phi \cdot \pi \cdot \sqrt{2} \cdot r_e \right)^{\frac{4}{3}} = 3,7712 \cdot 10^{-21} [s]$$

Division by t_{min} results in the jump number N_j

$$N_{j_x} = \frac{\left(\Phi \cdot \pi \cdot \sqrt{2} \cdot r_e \right)^{\frac{4}{3}}}{t_{min}} = 855,584$$

By multiplying by V_e we obtain a volume which we assume to be the spherical potential space of the electron, i.e. the space in which the electron is statistically distributed in the neutron and whose radius we can now simply calculate

$$V_x = N_{j_x} \cdot V_e = 1,075158 \cdot 10^{-45} [m^3]$$

$$r_x = \sqrt[3]{\frac{3V_x}{4\pi}} = 6,355181 \cdot 10^{-16} [m]$$

The sphere with the radius calculated above (see Fig. 2, dark blue circle) lies completely within the cube of the neutron and thus represents a useful basis for a neutron model.

What is really remarkable is that we can calculate the value N_{j_x} in a much simpler way than described above by starting from $N_{j_3} = k_{pe} = 1836.152$. The calculation itself is very simple, but the calculation steps are based on empiricism and not on profound theory.

$$N_{j_x} = \frac{k_{pe}}{\Phi f_{D42}^2 \sqrt{2}} = 855,583$$

We will return to this calculation in the more detailed consideration of time and distance (see last section).

4) Calculation of the average mass of the neutron

To calculate the potential energies, we need the distance of the electron's center of gravity from the positron's center of gravity. The maximum center of gravity distance results from the radius of the largest potential sphere r_x (see above) reduced by the radius of the electron r_e (see Fig. 2, black circle).

$$r_{max} = \sqrt[3]{\frac{3V_x}{4\pi}} - r_e = 5,68574855 \cdot 10^{-16} [m]$$

The minimum potential distance is $2r_e$. For the table below, the distance between the maximum and minimum distance was divided into 39 partial distances and the potential energy was calculated for the resulting 39 radii. The relative surfaces of the respective potential spheres are of particular importance, as they determine the weighting with which the individual energies are included in the total energy. The exact description of the individual columns is listed below Table 1.

0	5,6857474E-16	3,23277E-31	0,999999999	2,02883E-13	2,257373E-30	2,25737E-30	1,675790234E-27
1	5,5713558E-16	3,104E-31	0,960166751	2,07048E-13	2,303721E-30	2,21196E-30	1,675744818E-27
2	5,4569642E-16	2,97785E-31	0,921143051	2,11388E-13	2,352013E-30	2,16654E-30	1,675699402E-27
3	5,3425725E-16	2,85431E-31	0,882928901	2,15915E-13	2,402373E-30	2,12112E-30	1,675653986E-27
4	5,2281809E-16	2,73339E-31	0,8455243	2,20639E-13	2,454936E-30	2,07571E-30	1,675608570E-27
5	5,1137893E-16	2,61508E-31	0,808929249	2,25574E-13	2,509851E-30	2,03029E-30	1,675563154E-27
6	4,9993977E-16	2,4994E-31	0,773143746	2,30736E-13	2,567279E-30	1,98488E-30	1,675517737E-27
7	4,8850061E-16	2,38633E-31	0,738167793	2,36139E-13	2,627397E-30	1,93946E-30	1,675472321E-27
8	4,7706144E-16	2,27588E-31	0,704001389	2,41801E-13	2,690398E-30	1,89404E-30	1,675426905E-27
9	4,6562228E-16	2,16804E-31	0,670644535	2,47741E-13	2,756494E-30	1,84863E-30	1,675381489E-27
10	4,5418312E-16	2,06282E-31	0,63809723	2,53981E-13	2,825920E-30	1,80321E-30	1,675336073E-27
11	4,4274396E-16	1,96022E-31	0,606359474	2,60543E-13	2,898933E-30	1,7578E-30	1,675290657E-27
12	4,3130408E-16	1,86024E-31	0,575431267	2,67453E-13	2,975819E-30	1,71238E-30	1,675245241E-27
13	4,1986564E-16	1,76287E-31	0,545312609	2,74740E-13	3,056895E-30	1,66696E-30	1,675199825E-27
14	4,0842817E-16	1,66812E-31	0,516003501	2,82435E-13	3,142512E-30	1,62155E-30	1,675154409E-27
15	3,9698731E-16	1,57599E-31	0,487503942	2,90573E-13	3,233063E-30	1,57613E-30	1,675108992E-27
16	3,8554815E-16	1,48647E-31	0,459813932	2,99195E-13	3,328988E-30	1,53071E-30	1,675063576E-27
17	3,7410899E-16	1,39958E-31	0,432933472	3,08343E-13	3,430779E-30	1,4853E-30	1,675018160E-27
18	3,6266983E-16	1,31529E-31	0,40686256	3,18069E-13	3,538991E-30	1,43988E-30	1,674972744E-27
19	3,5123066E-16	1,23363E-31	0,381601198	3,28428E-13	3,654251E-30	1,39447E-30	1,674927328E-27
20	3,3979150E-16	1,15458E-31	0,357149386	3,39484E-13	3,777273E-30	1,34905E-30	1,674881912E-27
21	3,2835234E-16	1,07815E-31	0,333507122	3,51311E-13	3,908865E-30	1,30363E-30	1,674836496E-27
22	3,1691318E-16	1,00434E-31	0,310674408	3,63992E-13	4,049958E-30	1,25822E-30	1,674791080E-27
23	3,0547402E-16	9,33144E-32	0,288651243	3,77623E-13	4,201618E-30	1,2128E-30	1,674745664E-27
24	2,9403486E-16	8,64565E-32	0,267437627	3,92314E-13	4,365078E-30	1,16739E-30	1,674700247E-27
25	2,8259569E-16	7,98603E-32	0,247033561	4,08194E-13	4,541772E-30	1,12197E-30	1,674654831E-27
26	2,7115653E-16	7,35259E-32	0,227439044	4,25414E-13	4,733373E-30	1,07655E-30	1,674609415E-27
27	2,5971737E-16	6,74531E-32	0,208654076	4,44152E-13	4,941853E-30	1,03114E-30	1,674563999E-27
28	2,4827821E-16	6,16421E-32	0,190678657	4,64615E-13	5,169544E-30	9,85722E-31	1,674518583E-27
29	2,3683905E-16	5,60927E-32	0,173512788	4,87056E-13	5,419229E-30	9,40306E-31	1,674473167E-27
30	2,2539989E-16	5,08051E-32	0,157156468	5,11774E-13	5,694258E-30	8,94889E-31	1,674427751E-27
31	2,1396072E-16	4,57792E-32	0,141609697	5,39136E-13	5,998695E-30	8,49473E-31	1,674382335E-27
32	2,0252156E-16	4,1015E-32	0,126872475	5,69588E-13	6,337523E-30	8,04057E-31	1,674336919E-27
33	1,9108240E-16	3,65125E-32	0,112944803	6,03687E-13	6,716920E-30	7,58641E-31	1,674291503E-27
34	1,7964324E-16	3,22717E-32	0,09982668	6,42128E-13	7,144634E-30	7,13225E-31	1,674246086E-27
35	1,6820408E-16	2,82926E-32	0,087518106	6,85797E-13	7,630523E-30	6,67809E-31	1,674200670E-27
36	1,5676491E-16	2,45752E-32	0,076019081	7,35840E-13	8,187324E-30	6,22393E-31	1,674155254E-27
37	1,4532575E-16	2,11196E-32	0,065329606	7,93761E-13	8,831780E-30	5,76977E-31	1,674109838E-27
38	1,3388659E-16	1,79256E-32	0,05544968	8,61579E-13	9,586360E-30	5,31561E-31	1,674064422E-27

Table 1	I	II	III	IV	V	VI	VII
I	Distance of the spherical surface from the center r_{CO} (m)						
II	r_{CO}^2 (m ²)						
III	Relative surface sizes $O_{rel} = r_{COx}^2 / r_{COmax}^2$						
IV	Potential energy at distance $r_{CO} \rightarrow E_{OC}$ (J)						
V	Mass = E_{CO} / c^2 (kg)						
VI	Weighted mass $m_g = E_{OC} / c^2 \times O_{rel}$ (kg)						
VII	Neutron masses $m_{Ni} = m_g + m_p + m_e$ (kg)						

$$\sum_{i=1-39} m_{N_i} = 6,532216579 \cdot 10^{-26} [kg]$$

As we have introduced one electron into the model with each orbital used for the above calculation, we must of course divide by the number of electrons in order to obtain the average energy value for the one-electron system that corresponds to our model. In our opinion, the result of the calculation can be classified as very good.

$$\overline{m_{Ni}} = \frac{\sum_{i=1-39} m_{Ni}}{39} = 1,674927328 \cdot 10^{-27} [kg]$$

$$m_{N_{it}} = 1,674927498 \cdot 10^{-27} [kg]$$

$$\Delta_{rel} = 1 \cdot 10^{-7}$$

The function from column VII is linear, so that the first and last values from this column, for example, are sufficient for averaging. Nevertheless, we have chosen the more complex way to show that the neutron mass is not constant, but varies with time.

If we could measure a single neutron in the minimum time (t_{min}) we would obtain the different values listed in the table for repeated measurements. If we increase the measurement time to t_{per} , on the other hand, we obtain the average value, which of course we also obtain if we include a large ensemble of neutrons in the experiment, regardless of the measurement time, as is actually always the case in practice.

b) The calculation of the β -decay curve of the neutron

1) Calculation of the maximum and minimum energies of the decay spectrum

We first want to calculate the maximum and minimum kinetic energies, i.e. the energies to be expected in the decay spectrum, taking into account the dynamics of the system (oscillation model) for the large jump described in detail above. For the smallest jump, the effect is so small that it does not need to be taken into account.

The heaviest neutron is present when the electron is at a minimum distance ($2 r_e$) from the positron center.

$$m_{N_{max}} = 1,683119 \cdot 10^{-27} [kg]$$

From this, the edge length of the heaviest neutron can easily be calculated because the elementary particle density is constant.

$$V_{N_{max}} = \frac{m_{N_{max}}}{m_p} V_p = \frac{1,683119 \cdot 10^{-27}}{1,672621 \cdot 10^{-27}} 2,307345468 \cdot 10^{-45} = 2,321827238 \cdot 10^{-45} [m^3]$$

$$s_{N_{max}} = 1,324167647 \cdot 10^{-15} [m]$$

For the maximum distance of an electron in a corner of the neutron to the center, we need half the space diagonal RD_N , which results as follows:

$$\frac{1}{2} RD_{N_{max}} = \frac{1}{2} s_{N_{max}} \cdot \sqrt{3} = 1,146762821 \cdot 10^{-15} [m]$$

The distance from the center of a sphere with radius r_x in the corner of a cube to the tip of the corner is

$$r_x \cdot \sqrt{3}$$

This corresponds to half the space diagonal of a cube surrounding the electron. For the maximum distance of an electron from the center (see distance c - d in Fig. 4), the following therefore applies:

$$r_{x_{\max}} = \frac{1}{2} RD_{N_{\max}} - r_e \cdot \sqrt{3} = 1,0308137 \cdot 10^{-15} [m]$$

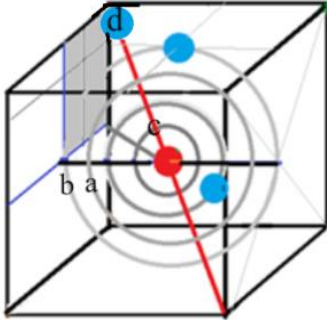


Fig. 4 Model of the neutron

The potential energy for the distance calculated above results:

$$E_{pot_{\min}} = \frac{e}{8\pi\epsilon_0 r_{x_{\max}}} = 698,46 [keV]$$

The potential energy for the smallest distance ($2r_e$) results:

$$E_{pot_{\max}} = \frac{e}{8\pi\epsilon_0 2r_e} = 5377,555 [keV]$$

$$\Delta E_{pot_{\max}} = E_{pot_{\max}} - E_{pot_{\min}} = 4679,1 [keV]$$

As explained above, only 1/6 of the potential energy is converted into kinetic energy of the electron.

$$E_{\max_{kin_{e^-}}} = \frac{(E_{pot_{\max}} - E_{pot_{\min}})}{6} = 779,849 [keV]$$

This result is surprisingly close to the value of 782.33 keV calculated using the mass difference between the neutron and the sum of the proton and electron. As already mentioned, the minimum jump energy is calculated without dynamic correction. The radius r_1 of the sphere in which the electron is statistically distributed (see above) and the radius r_2 of the sphere that is tangent to the center of the wall of the cube ($r_2 = s_{\min} / 2$) must be used. (Distance a - b in Fig. 4)

$$r_1 = 5,6857474 \cdot 10^{-16} \text{ m}$$

$$r_2 = 6,6070493 \cdot 10^{-16} [m]$$

$$\Delta E_{pot_{min}} = E_{pot_1} - E_{pot_2} = 1266,29 - 1089,72 = 176,57 [keV]$$

$$E_{kin_{min}} = \frac{(E_{pot_1} - E_{pot_2})}{6} = 29,43 [keV]$$

2) Calculation of the base curve

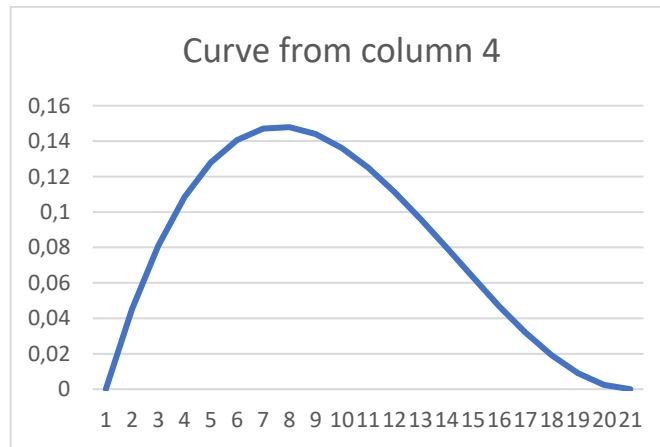
We now want to develop a simple model to derive a decay spectrum from this. To do this, we need to find out on which factors the frequency of the jumps from the spherical residence space of the electron around the positron to the surface of the neutron depends.

We assume that:

- the frequency of a jump or energy term depends on the size of the surface from which this jump originates
- the frequency of a jump depends on its energy, i.e. increases linearly with increasing energy

In Table 2, the radius 1 was assigned to the largest spherical shell and divided into 20 sub-steps. The associated relative surfaces can be represented by the relative distance squares (see column 2). Column 3 lists the relative energy terms, also normalized to 1, in ascending order, which, multiplied by the distance squares, give the total probability (column 4) for a particular energy term and are shown graphically in the adjacent diagram.

1	1	0	0
0,95	0,9025	0,05	0,045125
0,9	0,81	0,1	0,081
0,85	0,7225	0,15	0,108375
0,8	0,64	0,2	0,128
0,75	0,5625	0,25	0,140625
0,7	0,49	0,3	0,147
0,65	0,4225	0,35	0,147875
0,6	0,36	0,4	0,144
0,55	0,3025	0,45	0,136125
0,5	0,25	0,5	0,125
0,45	0,2025	0,55	0,111375
0,4	0,16	0,6	0,096
0,35	0,1225	0,65	0,079625
0,3	0,09	0,7	0,063
0,25	0,0625	0,75	0,046875
0,2	0,04	0,8	0,032
0,15	0,0225	0,85	0,019125
0,1	0,01	0,9	0,009
0,05	0,0025	0,95	0,002375
0	0	1	0



Tab 2

Fig.5

The above diagram was extended from 20 to 39 steps (see explanation below) and underlaid with a linear energy scale within the limits of the smallest and largest jump energies calculated above. The resulting curve is referred to below as the base curve.

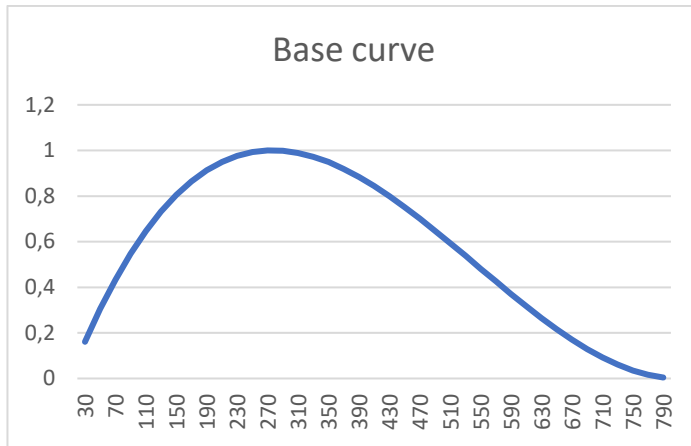


Fig. 6 Base curve: relative frequency (normalized to 1) of the energy terms (keV)

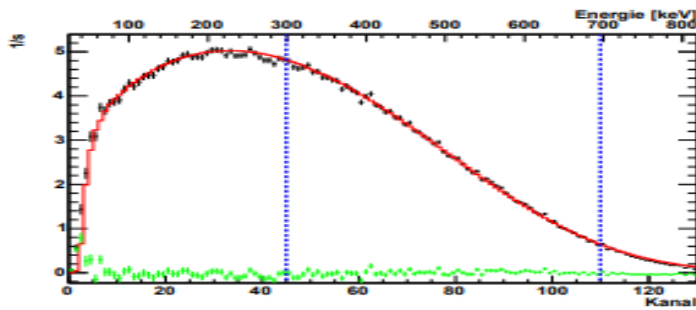


Fig.7 β -decay spectrum of the neutron (Ref 2)

Of course, the very simple spectrum constructed above (Fig. 6) does not exactly reflect the actual decay curve in Fig. 7, if only because the cubic shape of the neutron has not been taken into account so far. As a first approach, it should be shown here that a very simple model based on geometric and electrostatic considerations comes very close to the decay curve of the neutron without having to postulate any "ghost particles" such as neutrinos. However, one must be familiar with projection theory and understand that the interior of a neutron lies below the spatial resolution of our projection, in which the laws of physics as we know them only apply to a limited extent.

3) Calculation of the jump curve

A closer look at the curve in Fig. 7 suggests that it is a superposition of at least two different curves, whereby the asymmetry of the curve is, in our opinion, due to the coincidence of spherical and cubic symmetry in the neutron.

We have therefore divided the spherical residence space of the electron calculated above into 39 (780/20) spherical shells and calculated energy jumps from all shells to all points of the dark gray surface (see Fig. 8, blue arrows), which was resolved into 100 individual points, resulting in 39 x 100 energy values.

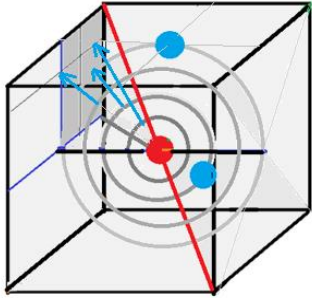


Fig. 8 Model of the neutron with dark gray target area

The gray area stands pars pro toto (x24) for the entire outer surface of the cubic neutron. Energy channels of 20 keV were selected (20 - 40, 40 - 60, etc.) and the calculated jump energies to be divided by 6 according to our findings above were assigned to these.

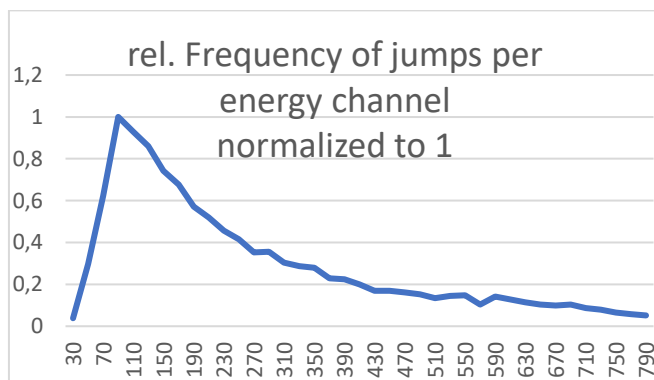


Fig. 9 Jump curve

The energy values 30, 50, 70 etc. on the abscissa correspond to the channels 20 - 40, 40 - 60, 60 - 80 etc.

Even with the most careful counting, the result is a rather strange curve with a very steep rise in the lowest energy range and an irregularly stepped curve that initially falls steeply and then flattens out in the high energy range (see Fig. 9)

4) Synthesis of jump and base curve

The base and jump curves normalized to 1 were superimposed (added) with different weightings in the following step.

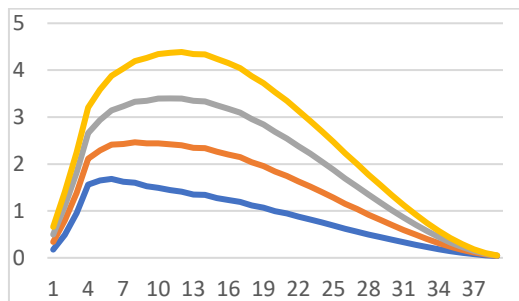


Fig. 10 Overlay of the base curve and the step curve with different weightings:
Base : Jump Blue 1:1 Red 2:1 Gray 3:1 Orange 4:1

A dedicated evaluation of the above curves showed that the gray curve (3:1) in fig 10 is in excellent agreement with the experimentally determined curve for the β -decay of the neutron (Fig. 11a)

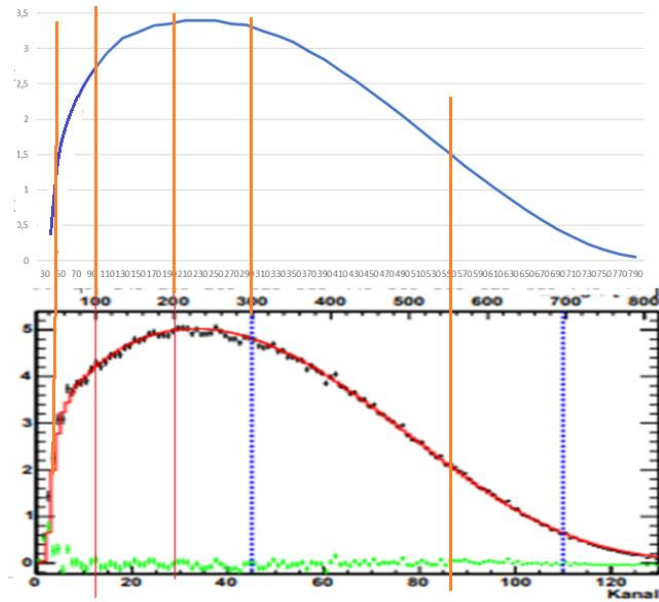


Fig. 11 a top: β -decay curve calculated in this work *
 Fig. 11 b bottom: Measurement curve of neutron decay (Ref. 2)
 black: measured values red: equalization curve

*The gray curve in Fig. 10 has only two fixed points in the lowest energy range, so that it drops almost linearly towards zero. Some additional data points were therefore used here and the curve was modified slightly accordingly.

The ratio 3:1 corresponds to the expectation, as we have the energy factor f_E and the distance factor of the spherical shells from the center f_{D0} in the system of equations for the base curve. The latter is included in the equation as a square, so that this equation is determined by the product of the three factors $f_E f_{D0} f_{D0}$. The jump curve only contains the distance f_{0F} from the electron orbitals to the surface of the neutron as a factor. In order to give equal weight to all factors in a superposition, the base and jump curves must therefore be superimposed in a ratio of 3:1.

In Fig. 11, the measurement curve (bottom) and the curve derived in this work (top) are overlaid to scale (x-axis).

The agreement between the curves is astonishingly precise. The overall shape of both curves is almost identical. Their maxima are exactly in the same range and the inflection points (right, orange bar) also match exactly.



Fig. 12 a

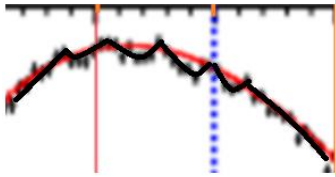


Fig. 12 b

If we take a closer look at the measurement curve in the area of the maximum (Fig. 12 b), we notice an unusually unsteady curve with a kind of zigzag pattern, which is particularly surprising in an area with the highest count rate, as such irregularities, which are normally caused by measurement technology, are more likely to be expected at low count rates, i.e. with a poor signal-to-noise ratio.

An almost identical pattern - albeit not as pronounced - but with exactly the same peaks and troughs at the same energy values, is also shown by the curve we calculated (see Fig. 12 a). In this area, the jump curve (Fig. 9) has its highest values and the unsteady, stepped course of this curve is still noticeable in the superposition.

If not only the measurement curve itself, but also such fine irregularities in a measurement curve are reproduced almost exactly in a theoretical curve derived from a simple model, it can be assumed that the model on which the calculation is based is correct.

Moreover, since this "jagged pattern" is precisely due to the collision of the spherical inner life (electron orbits) and the cubic outer surface of the neutron, the image of a **spherical neutron** consisting of quarks and gluons is obsolete. Above all, however, the "neutrino concept" is also no longer tenable, at least for the β -decay of the neutron, since neutrinos do not play the slightest role in the derivation of this curve.

c) The conversion from length to time and vice versa

1.) Basics

In the first sections, we repeatedly converted space into time and vice versa by simply exponentiating with $4/3$ or $3/4$ without giving an explicit explanation, which we will do here.

In an earlier paper (Ref. 3) we had established a connection between time and length.

$$S_x^{4/3} \equiv t_x \cdot S_x^{4/3} \xrightarrow{f} t_{\text{time}} \cdot (f \cdot t)_{\text{time}} \cdot S_x^{3/4} \xrightarrow{f} S_x$$

The above system of equations is based on the idea of projection theory that time is just another representation of our three-dimensional world in the fourth dimension.

In an isotropic space that is invariant to coordinate displacement, we can consider each distance to be composed of equal portions of each of the three spatial dimensions $s = (s_{x,y,z} = 1/3)^3$. We assume that we can extend this procedure to the 4th dimension and obtain a "time length" ($s^{4/3}$), which still has to be transformed into the world of our time measurement by means of a conversion factor (f_{time}).

2. Calculation of the time factor (f_{time1}) inside the neutron

Before we refresh the results of the above work, let us return to the inner life of the neutron. In section B 3.) we calculated the potential volume of the electron as the number of electron volumes in two fundamentally different ways. We will now use these equations to calculate the proportionality constant t_{min1} between time and length, which is valid **in the interior of the neutron**.

$$N_{j_1} = \frac{(\phi\pi r_e \sqrt{2})^{\frac{4}{3}}}{t_{min}} = 855,584$$

$$N_{j_2} = \frac{N_{j_3}}{\phi\sqrt{2}f_{d42}^2} = 855,583$$

$$N_{j_3} = k_{Pe}$$

Despite the small numerical difference, we set the two equations equal and introduce the proportionality factor f_{time1}

$$\frac{(\phi\sqrt{2}\pi r_e)^{\frac{4}{3}}}{t_{min}f_{time1}} = \frac{N_{j_3}}{\phi\sqrt{2}f_{d42}^2}$$

$$\frac{\phi\sqrt{2}f_{d42}^2 (\phi\sqrt{2}\pi r_e)^{\frac{4}{3}}}{t_{min}f_{time1}} = N_{j_3}$$

$$s_x = \phi\sqrt{2}\pi r_e = \phi\sqrt{s_{min}r_e} = 4,8123747 \cdot 10^{-16} [m]$$

The expression marked in red in the brackets in the above equations is the decisive base length for the further calculation. As the calculation shows, the length s_x is significantly less than the minimum length ($1.3214098 \cdot 10^{-15} m$) of our projection system and can therefore be assigned to the interior of the neutron.

We have replaced k_{Pe} with N_{j_3} above to make it clear that we are not dealing here with the weight ratio of proton to electron, but with the number of jumps or number of electron volumes required to completely fill the neutron interior, i.e. both the length s_x and the target quantity N_{j_3} are quantities that can be assigned to the interior of the neutron.

Since N_{j_3} is known, we can save ourselves the trouble of explicitly calculating the value and solve the equation directly for the proportionality constant f_{time1} , because this is the actual goal in this context.

$$f_{time1} = \frac{\phi\sqrt{2}f_{d42}^2 (\phi\sqrt{2}\pi r_e)^{\frac{4}{3}}}{t_{min}N_{j_3}} = 0,9999984 = \frac{1}{1,0000016} \left[\frac{m^{\frac{4}{3}}}{s} \right]$$

We are somewhat surprised to find that the proportionality constant is 1, which is significantly different from the value reported in Ref. 6.

3. Calculation of the time factor (f_{time2}) outside the neutron

Let us recapitulate the calculation from Ref. 6 and start from the definition equation for c (Ref. 4).

$$\frac{s_{\min}}{t_{\min}} = c$$

The base length is s_{\min} , i.e. a quantity that we can still measure and therefore cannot be assigned to the inside of a neutron. Similarly, the target value c has nothing to do with the inside of the neutron. In contrast to the calculation of f_{time1} , we convert the time here according to the equation below.

$$t_{\min} = \frac{r_e^{\frac{3}{4}}}{f_{time2}}$$

$$\frac{f_{time2} s_{\min}}{r_e^{\frac{4}{3}}} = c$$

$$f_{time2} = \frac{r_e^{\frac{4}{3}} c}{s_{\min}} = 61,668 \left[\frac{m^{\frac{4}{3}}}{s} \right]$$

The proportionality constant f_{time2} calculated here could be determined independently of the above equation in several ways (see Ref 3), so that the value calculated above is not a random value from a specific calculation, but an important universal constant in our world of time and space.

4. Summery and Conclusions

We introduced the conversion factor f_{time1} with the value 1 and the dimensions $m^{4/3}/s$ above. However, we can also look at the matter more drastically if we assume that there are no lengths at all inside a neutron. Lengths there are only mathematical fictions, the size of which can be calculated from the respective, actually existing times using the power $\frac{3}{4}$. Finally, as we have already established at the beginning of this paper, there are no longer any orbits in the neutron on which the electrons orbit around the positron, but only electron jumps in the minimum time, through which the electron statistically occupies a certain space (potential space) in a certain period of time t_{per} .

As an important conclusion, it should be noted that, as postulated at the beginning, other physical laws are at least partially valid inside the neutron than in the world outside, i. e. in the world with defined lengths.

References

¹Vanderhaeghen, M. ; Walcher, Th.: Long Range Structure of the Nucleon.

In: Nucl. Phys. News 21:1 (2011), pp. 14-22

² Inaugural dissertation, Manuela Mund, Ruprecht Karls University 2006

³ ViXra: 2112.0016

⁴ viXra:2104.0093 The Projection Theory: An Approach to the Theory of Everything